SAND2019-6840C

Investigating Typical Additive Manufacturing Defect Geometries using Physical Vapor Deposition Explosives as a Model System


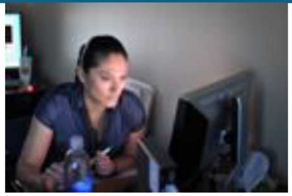
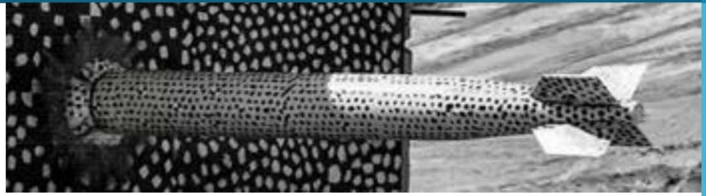

The 21st Biennial Conference of the American Physical Society Topical Group on Shock Compression of Condensed Matter, Portland, OR, June 16-21, 2019.

Caitlin O'Grady[a,b], Michael P. Marquez[a], Stephen Rupper[a], Jon Vasiliauskas[a], Robert Knepper[a], and Alexander S. Tappan[a]

[a]Sandia National Laboratories, Albuquerque, NM, 87185-1454
[b] Purdue University, West Lafayette, IN, 47907

Sandia National Laboratories is a multimission laboratory managed and operated by National Technology & Engineering Solutions of Sandia, LLC, a wholly owned subsidiary of Honeywell International Inc., for the U.S. Department of Energy's National Nuclear Security Administration under contract DE-NA0003525.
SAND2019-xxxx

Introduction and Motivation

- Additive Manufacturing (AM)
  - AM techniques use less material and produce less waste
  - Can be used to make complex geometries, custom parts
- Defects or artifacts could change the performance of the high explosive (HE)
- Robocasting can have variability between parts designed to be identical due to artifacts or defects
  - Investigate common AM defects or artifacts in the energetic material that result from Robocasting
    - Using Physical Vapor Deposition (PVD) explosive samples as a model system
    - Determine experimentally the extent to which AM artifacts could create hot spots and affect the shock/detonation front of a HE

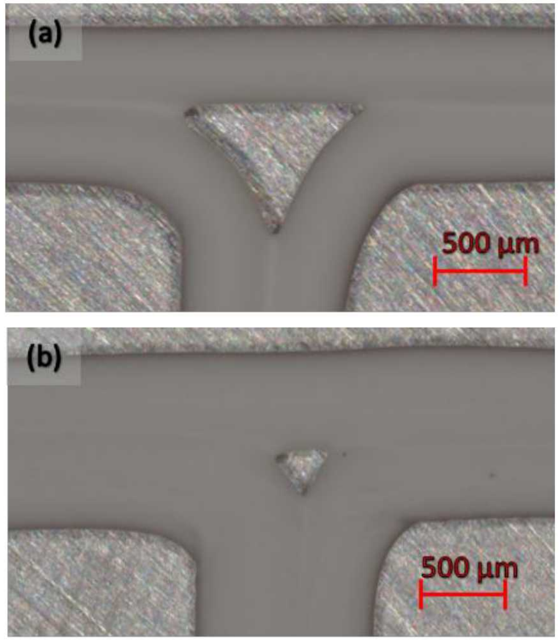

(Above Images) Optical micrographs of CL-20 based materials after robocasting that show common AM artifacts/defects, including (a) Large triangle void artifact and (b) small triangular void.

PETN Thin Films with Embedded Voids

- PVD allows for HE to be deposited with precise dimensions and patterned voids
  - A shadow mask defines the deposition area to ensure precise control of the HE dimensions as well as the void geometry.
    - Different shadow mask used to define the triangular void area on the substrates at different sizes.
    - Assembly consisted of bringing 2 substrates together to create triangular or diamond shaped voids.
      - It was observed that any gap between the 2 substrates would result in a failure to detonate

Optical microscope image of a 1 mm void on a confined substrate.

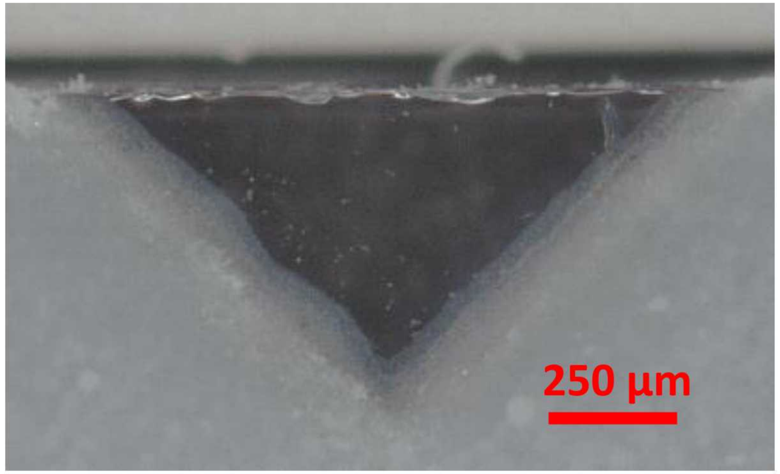

Proposed substrate setup with (left to right) optical micrograph of a 1 mm triangular setup, proposed 0.5 mm triangle-shaped void, another orientation of a 0.5 mm triangular void, and 0.5 mm diamond-shaped void.

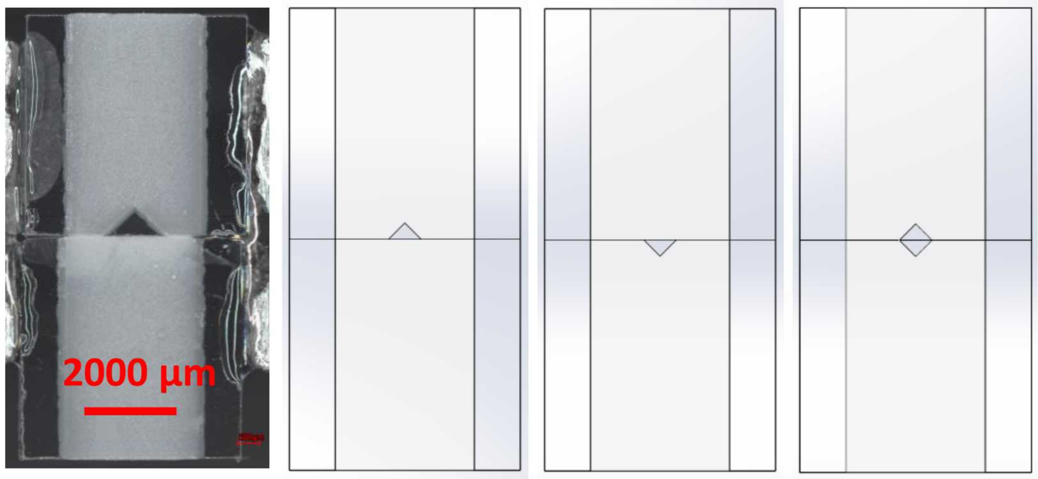

Framing Camera View

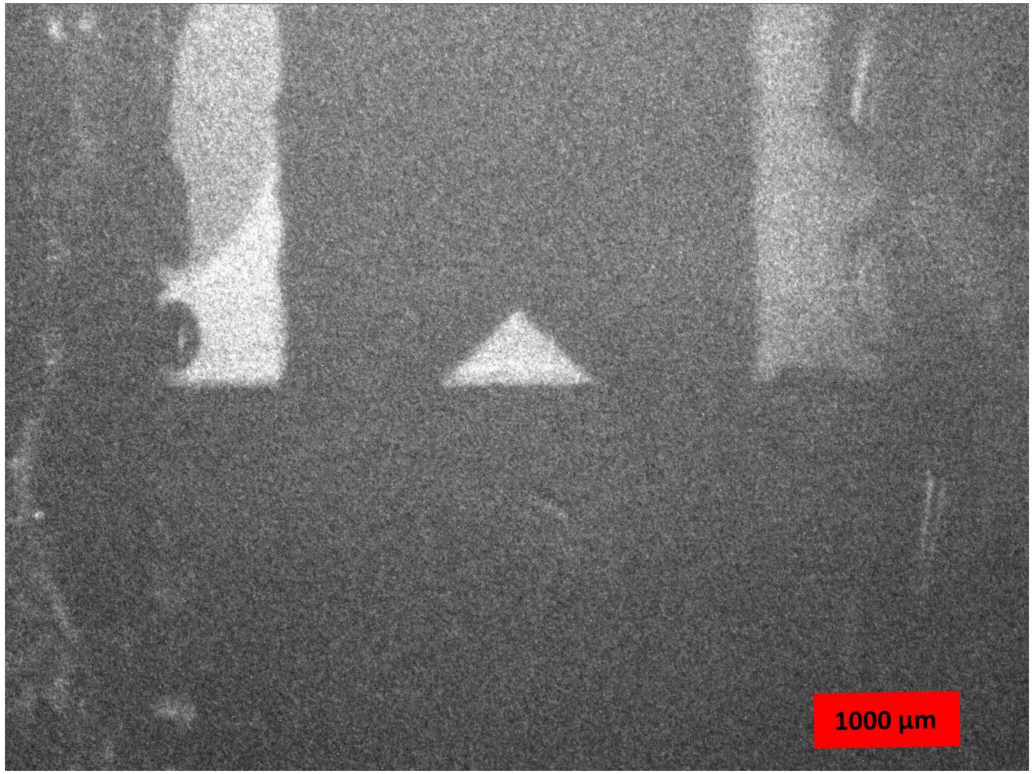

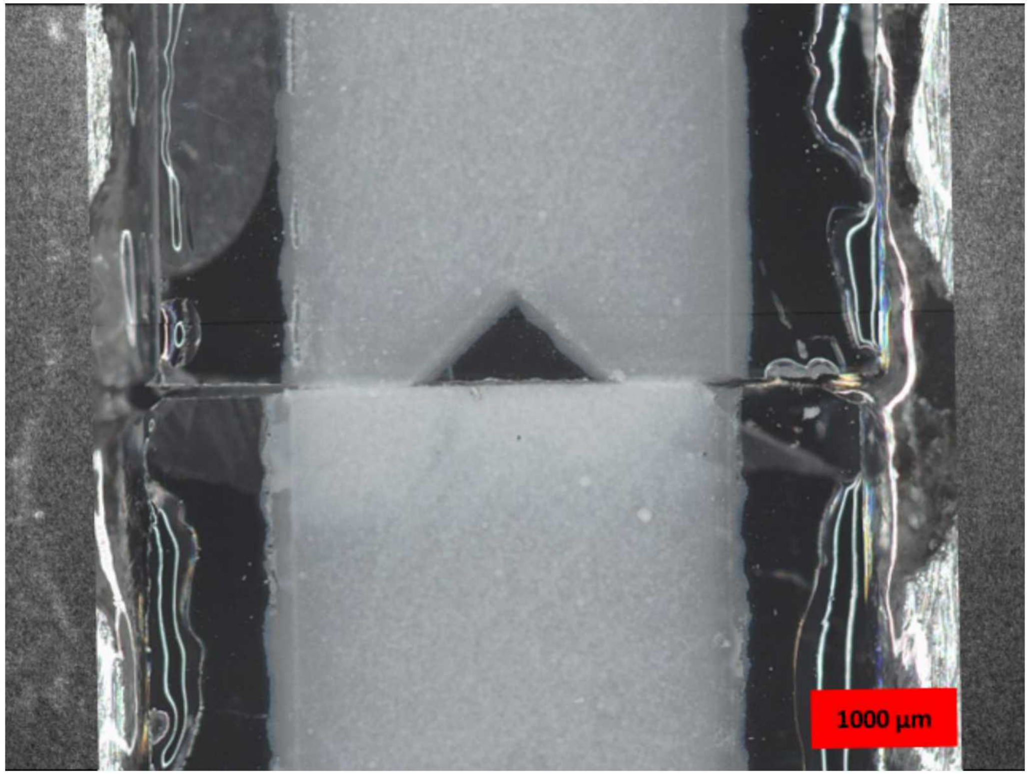

(Left) Static image (Frame 2) taken with framing camera prior to experiment. (Right) Optical microscope images (40× magnification) of same sample prior to the experiment.

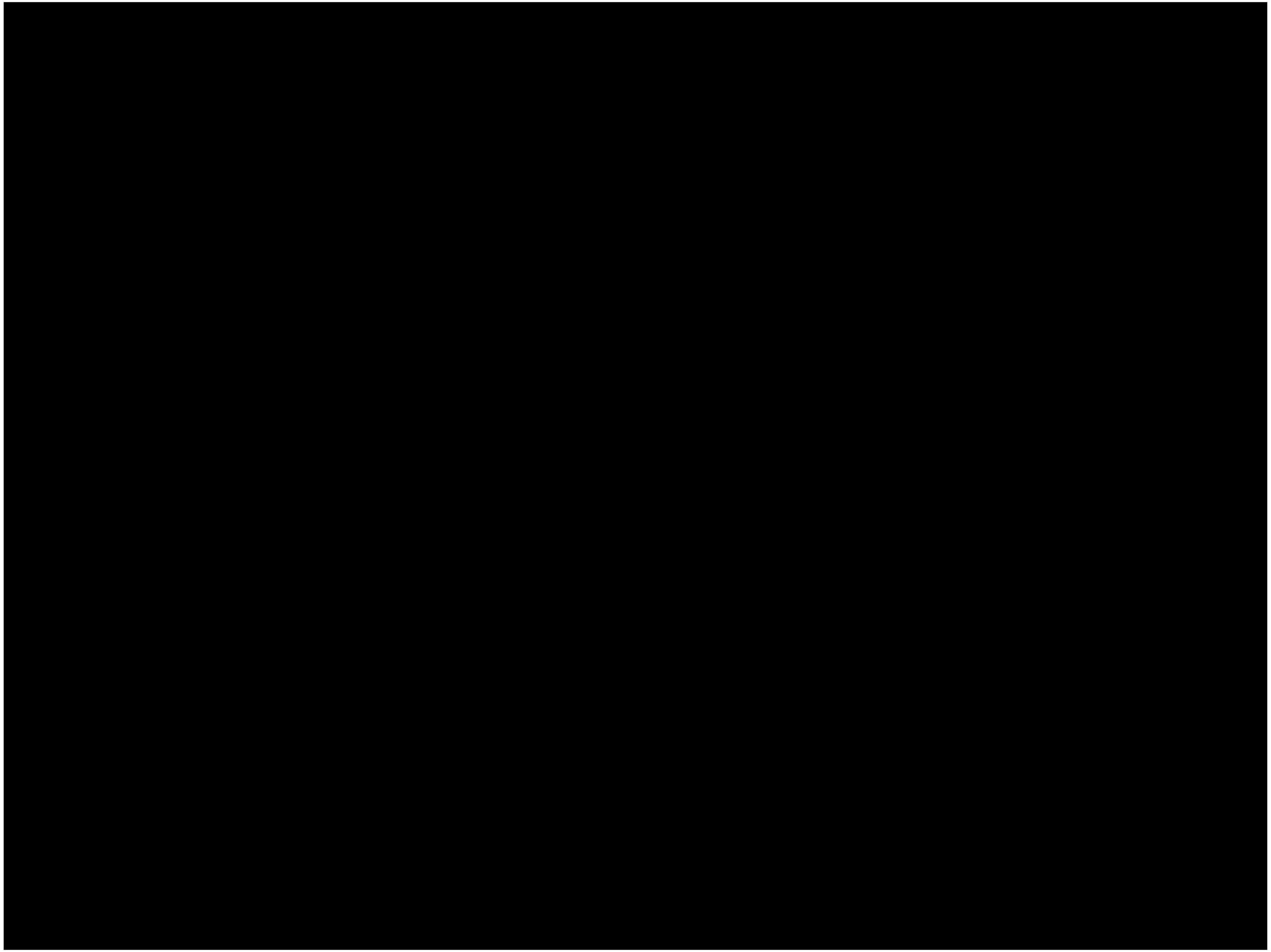

Images were recorded at 14 MHz (1/70 ns) with an exposure of 10 ns.

Dynamic Images

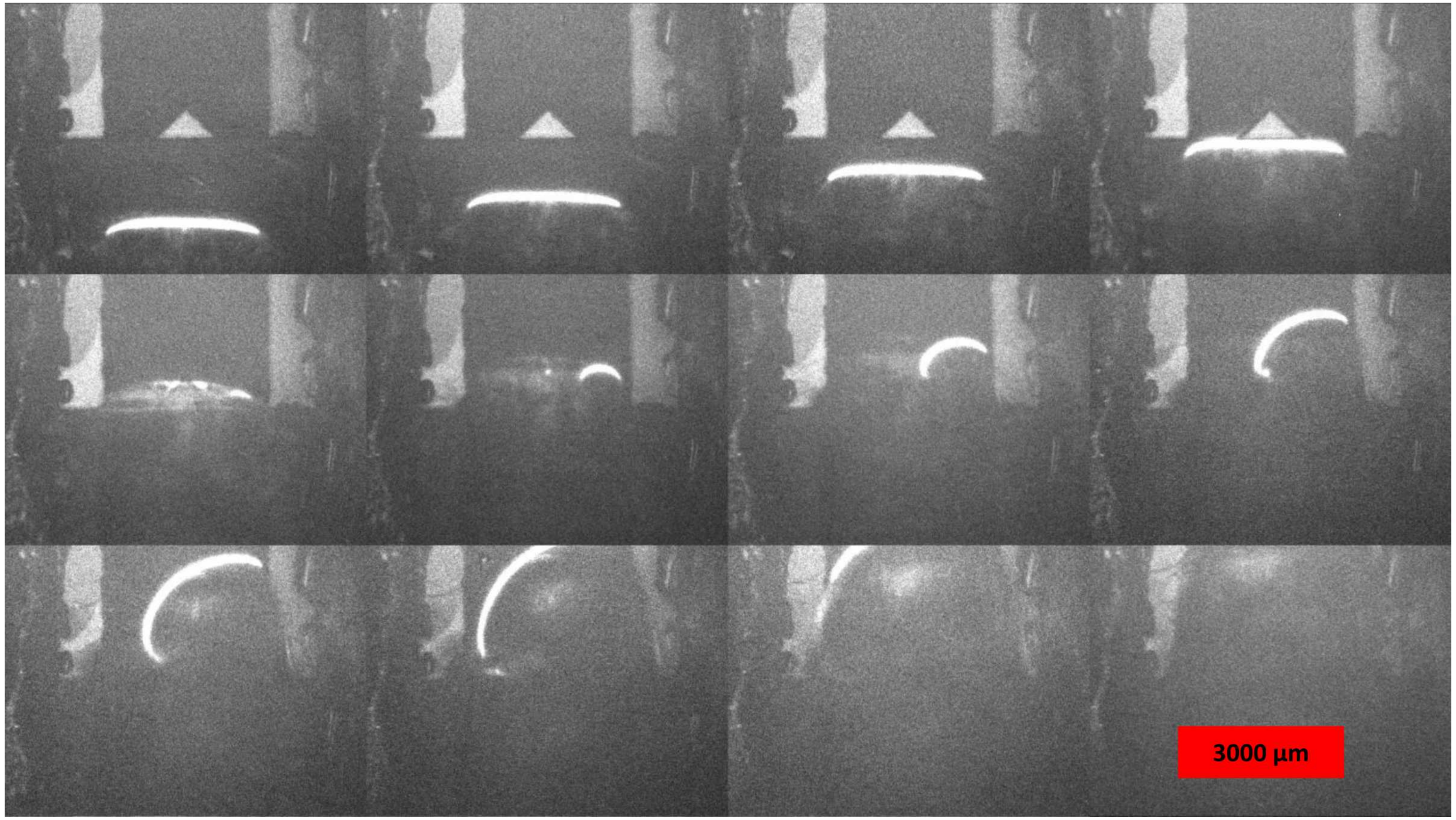

Images were recorded at 14 MHz (1/70 ns) with an exposure of 10 ns.

Detonation occurred through sample. Can observe the detonation front failed on one side upon contact with the void. The detonation front propagated around the void.

(Top Left to Right) Frames 4 to 7 overlaid on top of optical microscope image.
(Bottom Left to Right) Frames 8 to 11 overlaid on top of optical microscope image

SF = shock front
DF = detonation front
FD = failed detonation
LR = late reaction

Detonation failed at the left side of the gap. The shock front jetted across the void. The detonation propagated around the void, but failed in the damaged, or pre-shocked material.

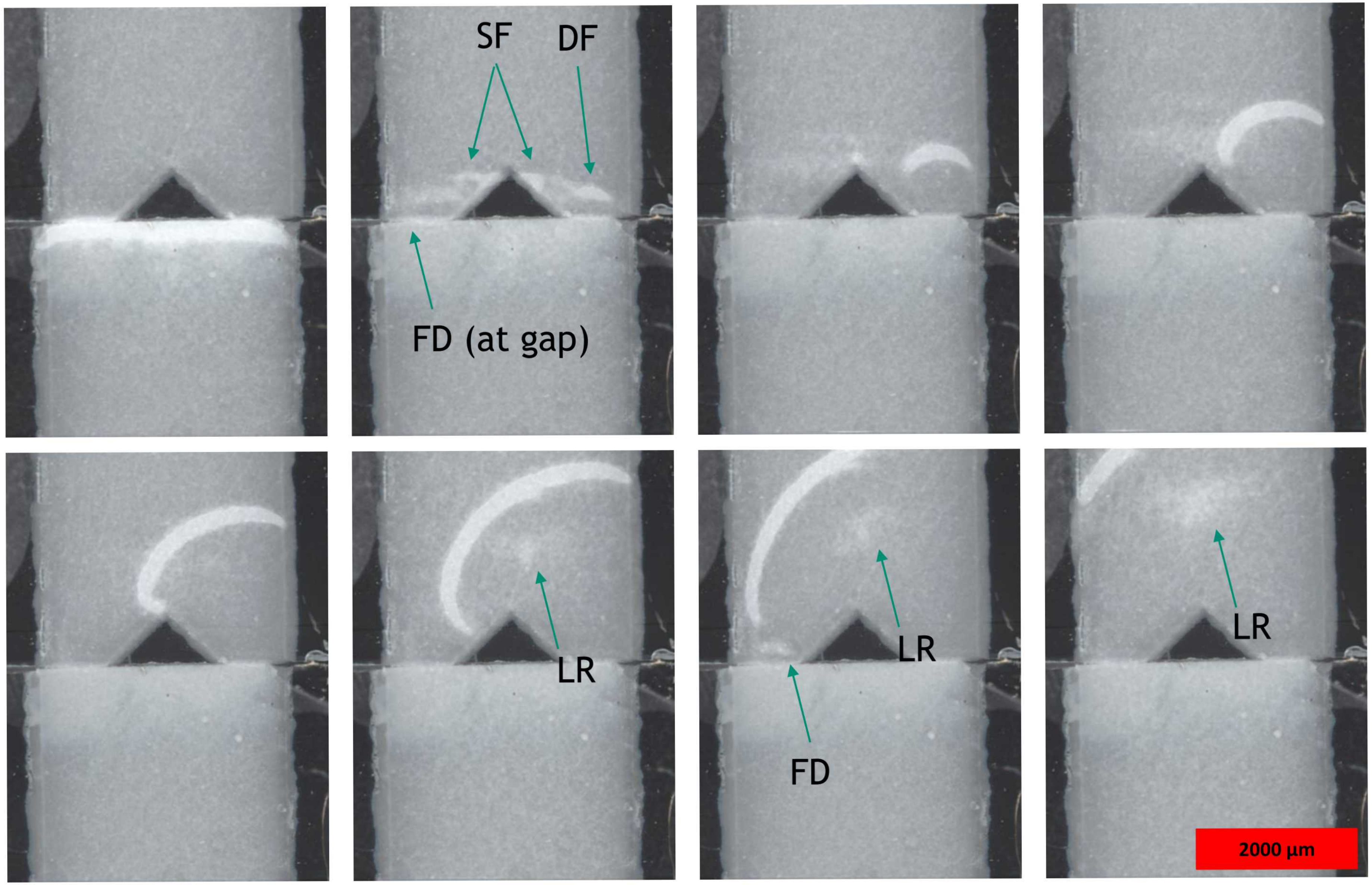

Micromushroom Test

- Determine deposition characteristics for the PETN such that the detonation corner turning is atypical
  - "Detonation corner turning" = ability of detonation front to propagate into unreacted explosive that is not within the normal path of the detonation front [1].
  - Goal is to evaluate corner turning properties as a function of deposition conditions
  - Corner turning likely has an effect on hot spot formation after a shock or detonation passes
- Test three different conditions:
  - Confined PETN slightly above critical detonation thickness
  - Confined PETN well above critical detonation thickness
  - Unconfined PETN well above critical detonation thickness

(Top) Processed framing camera images of PETN micromushroom tests with a stem width of 1.00 mm and a thickness of 277 µm [1]. The individual images from which these were taken with a 5 ns exposure time at 33 MHz (1/30 ns) [1].

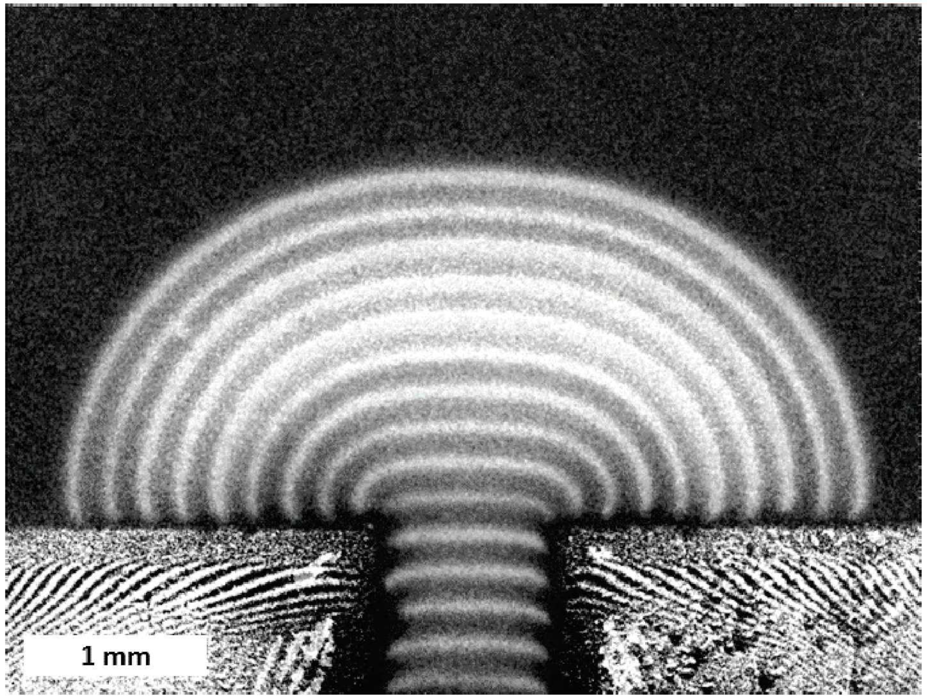

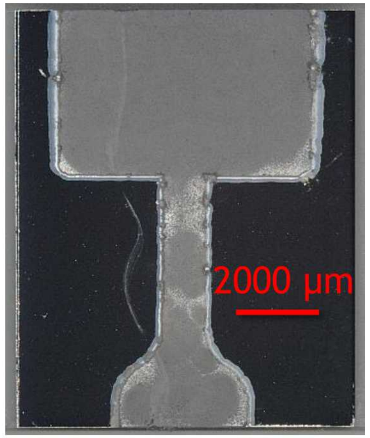

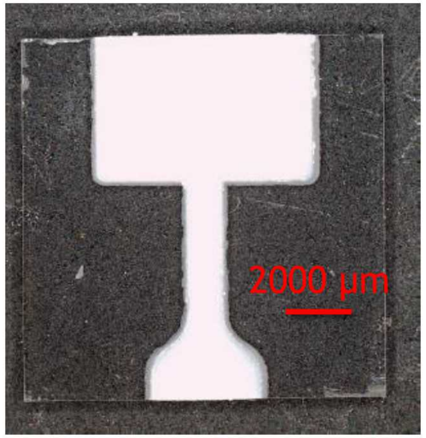

Optical micrograph of (Left) confined and (Right [1]) unconfined PETN micromushroom test sample. These samples are deposited on 1 cm polycarbonate substrates and have 1 mm wide stems.

[1] A. S. Tappan, C. D. Yarrington, and R. Knepper, Detonation corner turning in vapor-deposited explosives using the micromushroom test, *AIP Conference Proceedings,* **2018,** *1979*, 100041.

Conclusions

- Typical AM defects/artifacts should affect the detonation front of an HE
  - Both the size and shape of the void are likely to affect the detonation front
    - Jetting
    - Preshock in material ahead of detonation (compressed, rubblized)
    - Partial reaction
    - Detonation wave interaction after the void
- A gap between substrates causes detonation failure
- Future work
  - Developing a new configuration that would eliminate any potential gap between substrates
  - Computational models of the experiment

Acknowledgements

I would like to gratefully acknowledge:

- Ben Hanks for assistance with manufacturing
- Adrian Casias, Billy Cunningham, and Amanda Nicole Dean for assistance with deposition masks
- I would also like to thank my Purdue advisors Dr. Son and Dr. Chen for all of their help during this process

This project was funded in part by Purdue ONR MURI project and the Joint Department of Defense/Department of Energy Munitions Technology Development Program as well as Sandia's Laboratory Directed Research and Development program.

Questions?

Backup Slides

Optical Microscope Images of Assembly

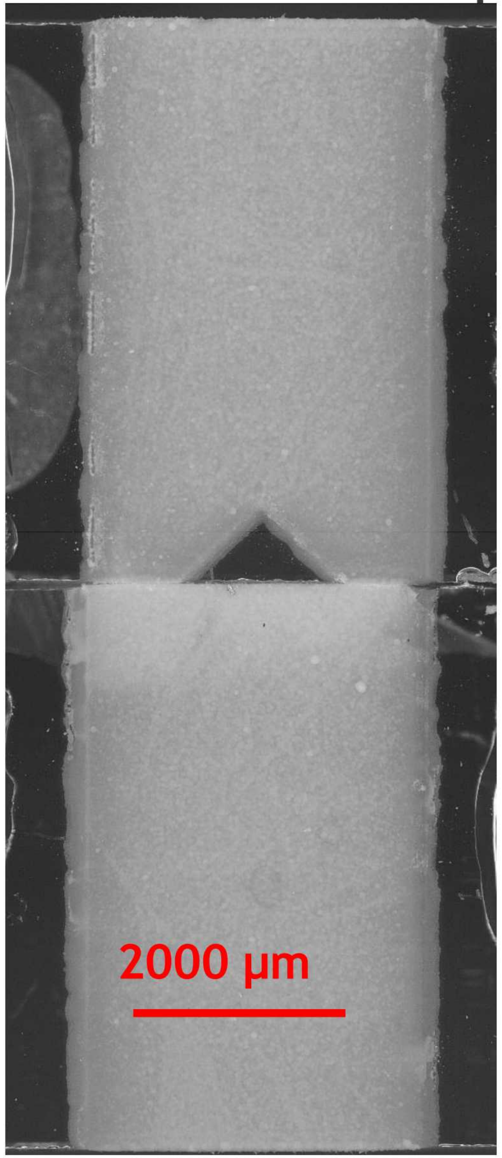

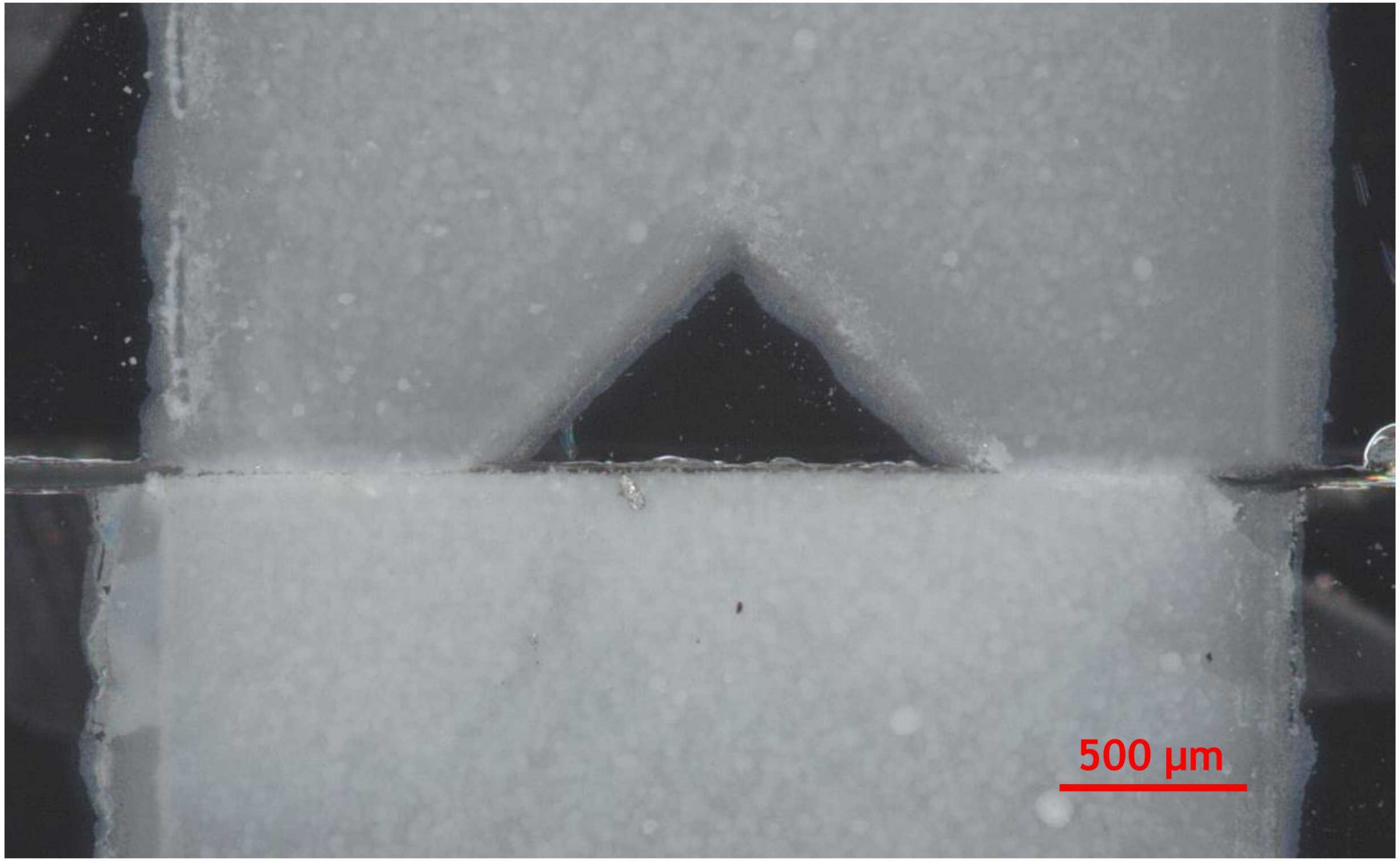

Optical microscope images (Left) at 40× and (Right) 80× magnification of the assembled experiment. A large triangular shaped void can be seen in the sample. The gap between the 2 samples has been minimized to prevent possible detonation failure.

Dynamic Images

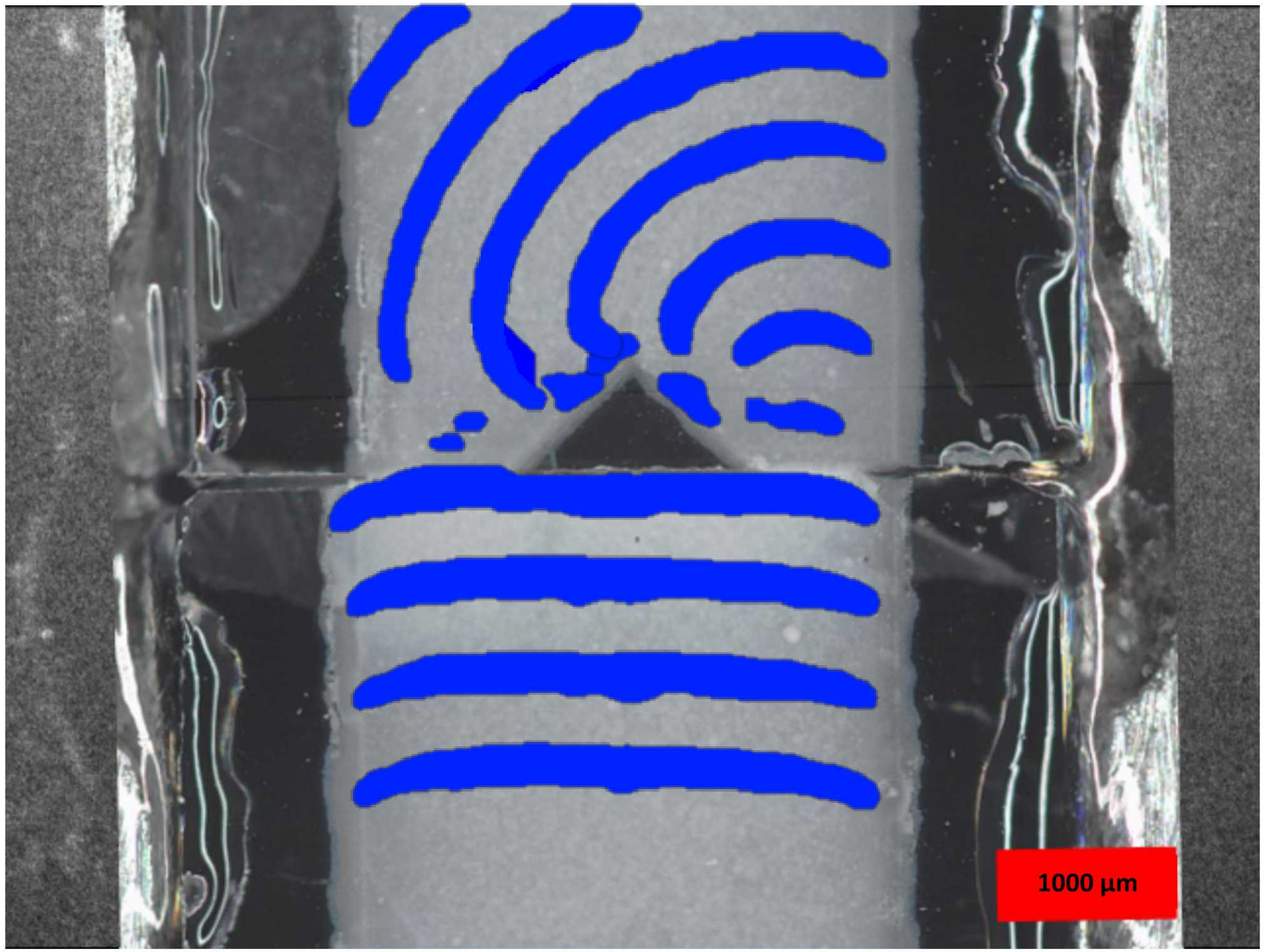

Images were recorded at 14 MHz (1/70 ns) with an exposure of 10 ns.

Composite Image showing the propagation of the detonation front during the experiment.

(Top Left to Right) Frames 4 to 7 overlaid on top of optical microscope image.
(Bottom Left to Right) Frames 8 to 11 overlaid on top of optical microscope image

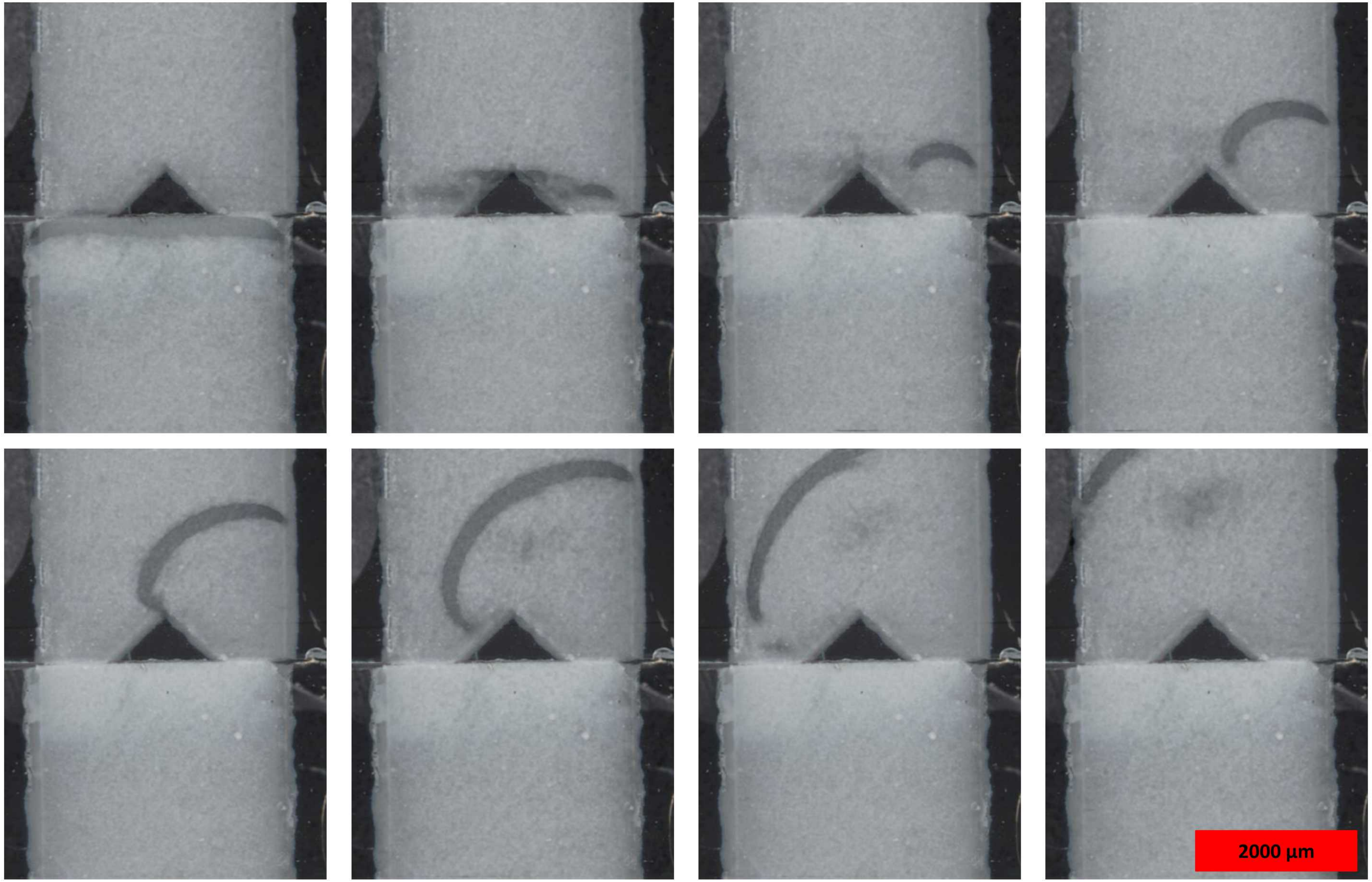

(Top Left to Right) Frames 4 to 7 overlaid on top of optical microscope image.
(Bottom Left to Right) Frames 8 to 11 overlaid on top of optical microscope image

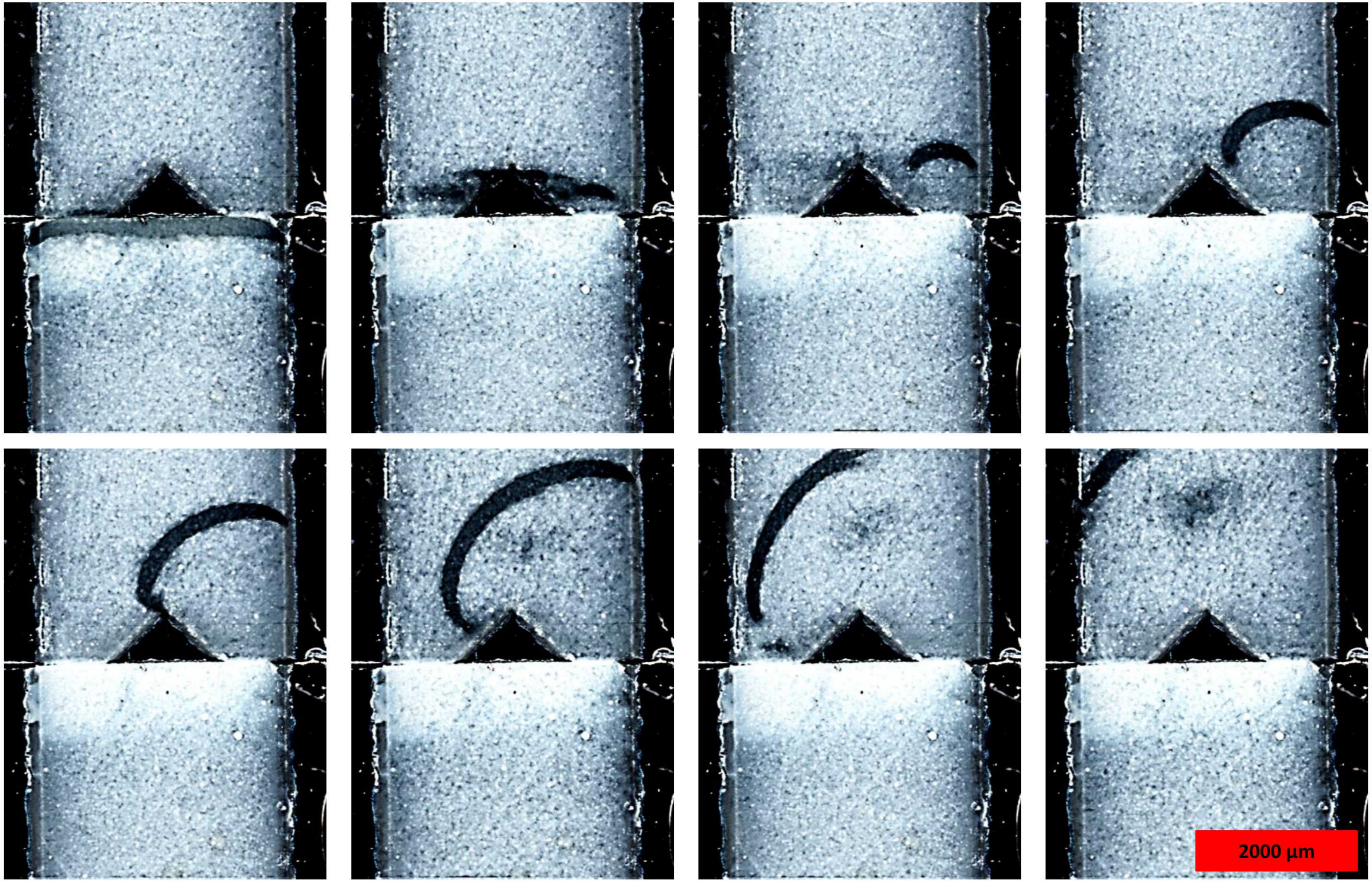

Frames 1 to 11 overlaid on top of optical microscope image. Detonation front can be observed as a line diagram

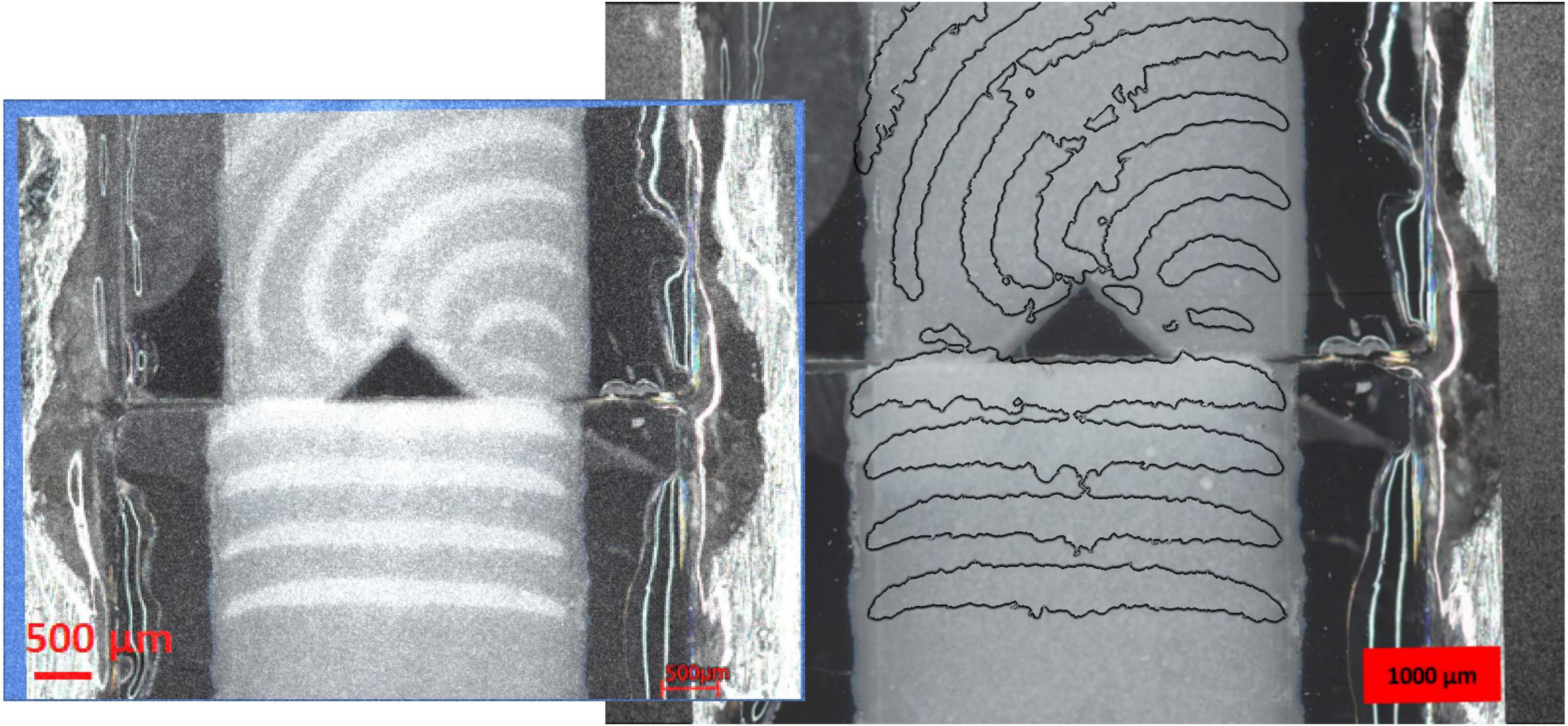

References

[1] J.-P. Kruth, M. C. Leu, and T. Nakagawa, Progress in additive manufacturing and rapid prototyping, *Cirp Annals,* **1998,** *47*, 525.

[2] M. Mani, K. W. Lyons, and S. Gupta, Sustainability characterization for additive manufacturing, *Journal of Research of the National Institute of Standards and Technology,* **2014,** *119*, 419.

[3] M. F. Smith, *Additive Manufacturing at Sandia*, Sandia National Laboratories, Albuquerque, NM, **2015**.

[4] J. E. Field, Hot spot ignition mechanisms for explosives, *Accounts of Chemical Research,* **1992,** *25*, 489.

[5] D. L. Bonnett and P. B. Butler, Hot-spot ignition of condensed phase energetic materials, *Journal of Propulsion and Power,* **1996,** *12*, 680.

[6] A. Mellor *et al.*, Research Needs and Plan for Energetic Material Hazard Mitigationt, *Combustion Science and Technology,* **1988,** *59*, 391.

[7] E. V. Roos, J. J. Benterou, R. S. Lee, F. Roseke, and B. C. Stuart, Femtosecond laser interaction with energetic materials, *High-Power Laser Ablation IV*, **2002**, *4760*, 415.

[8] L. Tran and H. Udaykumar, Simulation of void collapse in an energetic material, Part I: Inert case, *Journal of Propulsion and Power,* **2006,** *22*, 947.

[9] D. L. Damm, R. R. Wixom, and C. Yarrington, *Development of a Grain-Scale Model for Shock Initiation of HNS*, Sandia National Laboratories, Albuquerque, NM, **2014**.

[10] J. G. Bennett, K. S. Haberman, J. N. Johnson, and B. W. Asay, A constitutive model for the non-shock ignition and mechanical response of high explosives, *Journal of the Mechanics and Physics of Solids,* **1998,** *46*, 2303.

[11] C. M. Tarver, S. K. Chidester, and A. L. Nichols, Critical conditions for impact-and shock-induced hot spots in solid explosives, *The Journal of Physical Chemistry,* **1996,** *100*, 5794.

[12] F. P. Bowden and A. D. Yoffe, *Initiation and growth of explosion in liquids and solids*. CUP Archive, **1985**.

[13] H. Eyring, R. E. Powell, G. H. Duffy, and R. B. Parlin, The stability of detonation, *Chemical Reviews,* **1949,** *45*, 69.

[14] E. L. Lee and C. M. Tarver, Phenomenological model of shock initiation in heterogeneous explosives, *The Physics of Fluids,* **1980,** *23*, 2362.

[15] B. L. Holian, T. C. Germann, J.-B. Maillet, and C. T. White, Atomistic Mechanism for Hot Spot Initiation, *Physical Review Letters,* **2002,** *89*, 285501. 12/27/.

[16] J. A. Lewis, J. E. Smay, J. Stuecker, and J. Cesarano, Direct ink writing of three-dimensional ceramic structures, *Journal of the American Ceramic Society,* **2006,** *89*, 3599.

[17] J. A. Lewis, Direct ink writing of 3D functional materials, *Advanced Functional Materials,* **2006,** *16*, 2193.

[18] J. N. Stuecker, J. Cesarano III, and D. A. Hirschfeld, Control of the viscous behavior of highly concentrated mullite suspensions for robocasting, *Journal of Materials Processing Technology,* **2003,** *142*, 318.

References

[19] J. Cesarano III and P. D. Calvert, Freeforming objects with low-binder slurry, ed: Google Patents, **2000**.

[20] I. Cesarano and R. Segalman, Robocasting provides moldless fabrication from slurry deposition, *Ceramic Industry,* **1998,** *148*, 94.

[21] J. Cesarano, A review of robocasting technology, *MRS Online Proceedings Library Archive,* **1998,** *542*.

[22] J. E. Smay, G. M. Gratson, R. F. Shepherd, J. Cesarano III, and J. A. Lewis, Directed colloidal assembly of 3D periodic structures, *Advanced Materials,* **2002,** *14*, 1279.

[23] G. Mitteramskogler *et al.*, Light curing strategies for lithography-based additive manufacturing of customized ceramics, *Additive Manufacturing,* **2014,** *1*, 110.

[24] J. Wilkes, Y.-C. Hagedorn, W. Meiners, and K. Wissenbach, Additive manufacturing of ZrO2-Al2O3 ceramic components by selective laser melting, *Rapid Prototyping Journal,* **2013,** *19*, 51.

[25] S. A. Bernard, V. K. Balla, S. Bose, and A. Bandyopadhyay, Direct laser processing of bulk lead zirconate titanate ceramics, *Materials Science and Engineering: B,* **2010,** *172*, 85.

[26] E. Feilden, Additive manufacturing of ceramics and ceramic composites via robocasting, Doctor of Philosophy (PhD), Department of Materials, Imperial College London, **2017**.

[27] J. Hagan and M. Chaudhri, Fracture surface energies of high explosives PETN and RDX, *Journal of Materials Science,* **1977,** *12*, 1055.

[28] A. S. Tappan, C. D. Yarrington, and R. Knepper, Detonation corner turning in vapor-deposited explosives using the micromushroom test, *AIP Conference Proceedings,* **2018,** *1979*, 100041.

[29] R. Knepper, A. S. Tappan, R. R. Wixom, and M. A. Rodriguez, Controlling the microstructure of vapor-deposited pentaerythritol tetranitrate films, *Journal of Materials Research,* **2011,** *26*, 1605.

[30] A. S. Tappan, R. Knepper, R. R. Wixom, M. P. Marquez, J. P. Ball, and J. C. Miller, Critical detonation thickness in vapor-deposited pentaerythritol tetranitrate (PETN) films, *AIP Conference Proceedings*, **2012**, *1426*, 677.

[31] T. L. Andrew and T. M. Swager, A fluorescence turn-on mechanism to detect high explosives RDX and PETN, *Journal of the American Chemical Society,* **2007,** *129*, 7254.

[32] R. Knepper, R. R. Wixom, M. P. Marquez, and A. S. Tappan, Near-failure detonation behavior of vapor-deposited hexanitrostilbene (HNS) films, *AIP Conference Proceedings*, **2017**, *1793*, 030014.

[33] A. Tappan *et al.*, Patterning of regular porosity in PETN microenergetic material thin films, *Proc. 36th Int. Conf. ICT*, **2005**, 134.

[34] S. D. Herring, T. C. Germann, and N. Grønbech-Jensen, Dimensionality effects in void-induced explosive sensitivity, *Combustion Theory and Modelling,* **2016,** *20*, 866.

[35] S. D. Herring, T. C. Germann, and N. Grønbech-Jensen, Sensitivity effects of void density and arrangement in a REBO high explosive, *EPJ Web of Conferences*, **2010**, *10*, 00024.

[36] A. S. Tappan, R. R. Wixom, and R. Knepper, Critical Detonation Thickness in Vapor-Deposited Hexanitroazobenzene (HNAB) Films with Different Preparation Conditions, *Fifteenth International Detonation Symposium*, San Francisco, CA, **2014**, *1*, 5002.